

Oxidation of geraniol using niobia modified with hydrogen peroxide

Oxidación de geraniol utilizando niobia modificada con peróxido de hidrógeno

Jairo Cubillos ^{1*}, Jose J. Martínez ¹, Hugo Rojas ¹, Norman Marín-Astorga²

¹Grupo de Catálisis, Escuela de Ciencias Químicas, Universidad Pedagógica y Tecnológica de Colombia UPTC. Avenida Central del Norte 39-115. A.A. 150003 Tunja. Boyacá, Colombia.

²Eurecat U.S. Incorporated. 13100 Bay Park Rd. C.P. 77507. Pasadena, Texas, USA.

ARTICLE INFO:

Received: April 27, 2018

Accepted: April 16, 2019

AVAILABLE ONLINE:

April 22, 2019

KEYWORDS:

Niobium oxide, peroxo sites, regioselective

Óxido de niobio, sitios peroxo, regioselectividad

ABSTRACT: Nb_2O_5 bulk and Nb_2O_5 modified with H_2O_2 were studied in the epoxidation of geraniol at 1 bar and room temperature. The structural and morphological properties for both catalysts were very similar, indicating that the peroxo-complex species were not formed. The order of the reaction was one with respect to geraniol and close to zero respect to H_2O_2 , these values fit well with the kinetic data obtained. The geraniol epoxidation is favored by the presence of peroxo groups, which is reached using an excess of H_2O_2 . Moreover, the availability of the geraniol to adopt the three-membered-ring transition state was found as the best form for this type of compound.

RESUMEN: El óxido de niobio (niobia), Nb_2O_5 y Nb_2O_5 modificado con H_2O_2 fue explorado como catalizador en la epoxidación de geraniol a 1 bar y temperatura ambiente. Las propiedades estructurales y morfológicas de ambos catalizadores fueron muy similares, lo cual sugiere que no se formaron especies de complejo peroxo. El orden de la reacción fue uno con respecto a geraniol y cercano a cero con respecto al H_2O_2 . Estos valores son consistentes con los datos cinéticos obtenidos. La epoxidación de geraniol fue favorecida en presencia de grupos peroxo, que se alcanzan utilizando un exceso de H_2O_2 . Además, se encontró que, bajo las condiciones de reacción utilizadas en este trabajo, el geraniol fácilmente adoptó un estado de transición de un anillo de tres miembros como la estructura más favorable para este tipo de compuesto.

1. Introduction

Oxidation is one of the most important synthetic routes for the conversion of chemical compounds into valuable intermediates and products for the chemical industry. During the last decade, the peroxo and hydroperoxo complexes with different transition metals, including W, V, Mo, Ti and Nb, has drawn attention due to their exceptional catalytic activity in the oxidation of alkenes, aliphatic and aromatic hydrocarbon compounds [1, 2]. However, most of these works take place via homogeneous catalysis [3–5], which makes the catalytic process more expensive and difficult to execute and separate the products and catalyst, especially at large scale [6, 7].

The use of an environmentally friendly oxidant such as aqueous hydrogen peroxide (H_2O_2), as a modifier on heterogeneous catalysts to make easily recyclable

catalyst will be a challenging goal for the fine chemical industry. The catalytic technology target in this work using hydrogen peroxide as a surface modifier is developing large active sites, which can be applied for the oxidation of larger molecules. For niobia (Nb_2O_5) bulk, it is possible to improve the oxidizer properties just with a simple modification of Nb_2O_5 surface by treatment the solid with hydrogen peroxide (H_2O_2) [8–11]. The modified niobia shows high activity in the oxidation of cyclohexene [12], geraniol [13], and during the oxidation/dehydration of methanol to obtain dimethoxymethane [14]. In a previous work, we report the highly selective epoxidation of geraniol using Nb_2O_5/SiO_2 and $Nb_2O_5/MCM-41$ as heterogeneous catalysts [15], now we intended to verify the formation of peroxo sites from of the surface modification of Nb_2O_5 with H_2O_2 . This kind of surface modifications can produce a relative high concentration of peroxo groups on the surface [4, 16], this phenomenon occurs after a prolonged interaction between the niobia with the oxidant (H_2O_2) via a donor-acceptor mechanism to produce $Nb^{5+\delta-}$ species on the Nb_2O_5 surface [17]. The peroxo groups are the catalytically active species

* Corresponding author: Jairo Cubillos

E-mail: jairo.cubillos@uptc.edu.co

ISSN 0120-6230

e-ISSN 2422-2844



responsible of the oxygen transfer from the catalyst until the substrate. However, peroxyoniobate ($\text{Nb}(\text{O}_2)_4^-$) compounds are formed at the same time, which can be isolated using alcohol solutions. In general, the formation of these homogeneous species can help to enhance the catalytic activity.

Olefins epoxidation is a widely-used transformation in the fine chemical industry. Epoxides are valuable building blocks and versatile commercial intermediates owing to the numerous reactions they may undergo. During the epoxidation reaction, it is important to eliminate the acidity of the catalytic material to control the selectivity towards epoxide. H_2O_2 is an attractive option as an oxidant that can epoxidize different compounds in the presence of various transition metal-containing catalysts, obtaining just water as a by-product. Another favorable advantage is the use of heterogeneous catalysts for easy separation from products and regeneration in some cases. Therefore, the development of heterogeneous catalytic systems for oxidation reactions using H_2O_2 as oxidant is highly demanded. In this aspect, the development of recyclable oxidation catalyst with high catalytic performance is a key issue.

The mode of the oxidant activation on the catalyst surface determines the selectivity and the formation of peroxy sites, these play an important role during the oxidation reactions [14]. In this paper, the oxidation of geraniol was examined over Nb_2O_5 treated previously with H_2O_2 for understanding the catalytic behavior and the nature of the active sites in Nb_2O_5 .

2. Experimental section

2.1 Chemicals

The following compounds were used: Niobium (Nb_2O_5) (Sigma-Aldrich > 99.9%), $\text{NH}_3 \cdot \text{H}_2\text{O}$ (J.T. Baker, 37%), H_2O_2 (Fluka, 30%), geraniol (Sigma-Aldrich > 98%) and methanol (Sigma, > 99.8%). All chemicals were high-grade products and used without further purification.

2.2 Catalysts preparation

The Nb_2O_5 was used without further treatment. A peroxyoniobate Ammonium tetraperoxyoniobate ($(\text{NH}_4)_3^+[\text{Nb}(\text{O}_2)_4]^-$) was synthesized using the procedure reported by [6]. The obtained solid was labelled as $\text{Nb}_2\text{O}_5/\text{H}_2\text{O}_2$. In a typical procedure, Nb_2O_5 (1 g) in distilled water (25 mL) with a 35 wt.% solution of H_2O_2 (25 ml) and ammonia (6 ml, 25 wt.% solution) were placed in a round bottom flask. The mixture was stirred for a few hours. When the solid was totally dissolved, acetone was

added dropwise (100 ml) under stirring, a white precipitate was formed, which was filtered, washed with acetone and air-dried.

2.3 Catalysts characterization

The textural properties of the catalysts were determined by nitrogen adsorption at 77K using the conventional technique on Micromeritics ASAP 2020 equipment. The surface area was calculated using a multipoint Brunauer-Emmett-Teller (BET) model. The pore size distribution was obtained by BJH model, the total pore volume was estimated at a relative pressure of 0.99.

The XRD patterns were obtained on a PANalytical X-Pert-Pro diffractometer using Ni filtered and $\text{Cu } k\alpha$ radiation. Raman Spectra were obtained by Jobin-Yvon equipment model T64000 with a detector CCD. Spectra for each solid were taken over the range of 100 – 900 cm^{-1} , scanning at a step size of 1.0 cm^{-1} with an integration time constant of 1 s.

The XPS data were obtained in a Thermo Scientific Escalab 250 XI spectrometer. Measurements were performed at room temperature with monochromatic Al $K\alpha$ (h ν = 1486.6 eV) radiation. The analyzer was operated at 25 eV pass energy and a step size of 0.05 eV. To ensure that the ambient oxygen does not interfere with the sample analysis, the solids were first degassed in a *vacuum* pre-chamber of 10^{-7} mbar, and then the work *vacuum* is adjusted in the analytical chamber at a value of 6.3×10^{-9} mbar. C 1s signal (284.6 eV) was used as internal energy reference in all the experiments. Determination of core-level peak positions was accomplished after background subtraction per Shirley using peak XPS software. Peaks in a spectrum were fitted by a combination of Gauss and Lorentz curves, which also allowed separating overlapping peaks.

2.4 Catalytic activity evaluation

Catalytic reactions were performed in a low-pressure glass reactor equipped with a magnetic bar. Nb_2O_5 or $\text{Nb}_2\text{O}_5/\text{H}_2\text{O}_2$ (10 mg) and H_2O_2 (30%wt, 1 mmol) were placed into the reactor under N_2 at 400 rpm for 2 h at room temperature. The inert atmosphere was necessary to avoid the presence of molecular oxygen as oxidant. Then geraniol, was added, the mixture was maintained for 4 h under nitrogen atmosphere under agitation. The reaction mixture (catalyst, geraniol and H_2O_2) was diluted with distinct solvents (2 ml), and then the solution was separated from the catalyst by simple filtration. The effect of geraniol concentration was studied in the concentration range of 0.25 to 3 mmol. The temperature was varied from 293 to 333 K and the $\text{Nb}_2\text{O}_5/\text{H}_2\text{O}_2$ weight from 4 to 10

mg. To prevent any mass-transfer resistance, the catalyst particle sizes around 100 μm and stirring rates from 200 to 600 rpm were used.

The reaction mixture quantification and identification were performed by a Varian 3800 gas chromatograph equipped with Saturn 200 mass detector and a capillary column β -DEX (30 m x 0.25 mm). The relative peak area of substrates and products using a normalization method determined the conversion and selectivity. For this, a comparison between elution times of the reaction products with authentic samples was performed.

3. Results and discussion

3.1 Catalyst characterization

Surface area, pore size distribution and pore volume were determined from nitrogen adsorption/desorption isotherms (see Figure 1). Figure 1 shows the isotherms obtained for Nb_2O_5 and $\text{Nb}_2\text{O}_5/\text{H}_2\text{O}_2$ catalysts, which are type IV with H1 desorption hysteresis loop. The late and steep adsorption step shows the relatively large pore size and narrow pore size distribution (PSD); this type of hysteresis loop is associated with structured porous materials, consisting of spherical cavities with fairly regular array, and narrow PSD. Table 1 details the textural parameters determined by N_2 physisorption, including BET surface area, pore size and pore volume. Both samples show similar textural properties and no differences were observed after the treatment with H_2O_2 suggesting that the treatment with H_2O_2 does not have any effect on the morphological properties of the catalysts studied.

Table 1 N_2 physisorption data obtained from catalysts synthesized

Catalysts	S_{BET} , m^2/g	Pore volume, ml/g	Pore size, nm
Nb_2O_5	3.5	0.009	10.2
$\text{Nb}_2\text{O}_5/\text{H}_2\text{O}_2$	3.9	0.010	10.7

The morphological features of Nb_2O_5 and $\text{Nb}_2\text{O}_5/\text{H}_2\text{O}_2$ catalysts are presented on Figure 2. X-ray diffraction (XRD) patterns of the catalysts confirmed the crystalline and well-defined structure of Nb_2O_5 . The presence of Nb_2O_5 crystallites is confirmed for both samples showing diffraction peaks at $2\theta = 22.5^\circ, 28.5^\circ, 36.7^\circ, 46.1^\circ, 50.7^\circ, 55.2^\circ$ and 56.1° assigned to the crystal planes (001), (100), (101) (002), (110), (102) and (111), respectively. It was also shown that the porosity and hexagonal structure of Nb_2O_5 and $\text{Nb}_2\text{O}_5/\text{H}_2\text{O}_2$ ($T - \text{Nb}_2\text{O}_5$, JCPDS card # 28-0317) catalysts remained intact

after hydrogen peroxide treatment in agreement with N_2 desorption/adsorption results (see Table 1). No evidence was observed for a good match with the experimental and the theoretical powder diffraction patterns calculated by [18] for $(\text{NH}_4)_3[\text{Nb}(\text{O}_2)_4]$ which was synthesized using the same H_2O_2 method. Although, peroxy species complexes are formed, they were not capable of modifying the structural and textural properties, which is in agreement with the N_2 -physisorption results.

The surface composition of $\text{Nb}_2\text{O}_5/\text{H}_2\text{O}_2$ catalyst was determined by X-ray photoelectron spectroscopy (XPS). Figures 3a and 3b illustrate the deconvolution curves of O 1s and Nb 3d core levels. The Nb 3d spectra (Figure 3a) were deconvoluted using triplet lines attributed to Nb^{+5} phases [19, 20]. The binding energy of Nb $3d_{5/2}$ and Nb $3d_{3/2}$ lines was equal to 206.6 and 209.2 eV, respectively, with accuracy of ± 0.1 eV. The O 1s spectral line consisted of one doublet (Figure 3b) of different oxygen phases, attributed to oxygen atoms associated at two chemical bonds. The peak located at 529.9 eV corresponds to Nb-O bond and the peak close to 532 eV attributed to the formation of additional oxygenated groups on the surface of the catalyst. It is indicated that the peroxy group formation could be observed analyzing the region between 500 – 540 eV in the XPS spectrum [4, 15, 20]. They found that the peak around 532 eV was not observed for the commercial or synthesized Nb_2O_5 sample [4, 19]. There are two views about XPS of niobium oxides data in the literature. One group of authors claims that the peaks at 206 eV and at 205.4-205.6 eV correspond to $3d_{5/2}$ peaks of Nb^{+5} and Nb^{+4} , respectively [21, 22], while another group assigns them to Nb^{+4} and Nb^{+3} [23, 24]. Our interpretation agrees with that of the first group. Based on the empirical relationship ($\Delta(O - \text{Nb})$) between O 1s and Nb $3d_{5/2}$, it is possible to corroborate that the oxidation state of peroxoniobate is Nb^{+5} [25].

Raman spectroscopy was used to determine the vibration and rotation information in relation to the chemical bonds and symmetry in the $\text{Nb}_2\text{O}_5/\text{H}_2\text{O}_2$ structure, to find the finger print region of the spectra. In Figure 4, the Raman spectra of $\text{Nb}_2\text{O}_5/\text{H}_2\text{O}_2$ catalyst is shown. The spectrum displays the intensities of the Nb-O bending modes between 600-700 cm^{-1} corresponding to Nb_2O_5 structure. The broad peak detected at 694 cm^{-1} confirms the presence Nb_2O_5 in agreement with XRD analysis. A similar spectrum has been reported by [26]. They associated the broad band at 694 cm^{-1} with the formation of T- Nb_2O_5 phase. The T- Nb_2O_5 phase consists in 4×4 blocks that form the corner-shared octahedral of NbO_6 , each block is connected sharing the edges of the octahedron [27].

The high intensity observed in the band at 694 cm^{-1} for the

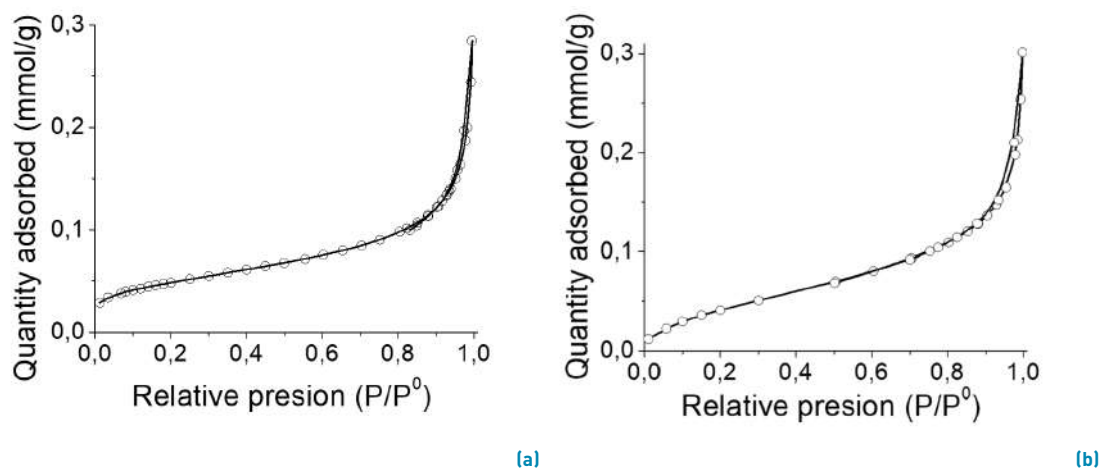


Figure 1 Nitrogen adsorption-desorption isotherms of solids: Nb_2O_5 bulk (left) and (b) Nb_2O_5/H_2O_2 (right)

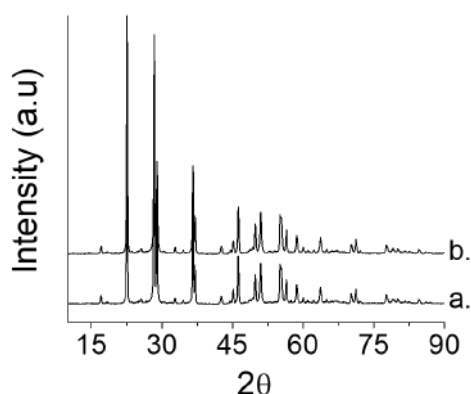


Figure 2 X-ray diffraction pattern of catalysts: (a) Nb_2O_5 bulk and (b) Nb_2O_5/H_2O_2 synthesized

Nb_2O_5/H_2O_2 catalyst, could be due to the extensive edge sharing of the octahedral. The bending vibrations at 540, 456 and 375 cm^{-1} are associated to distortions that may result in significant variations in the Nb-O lengths. Raman band between 300 and 150 cm^{-1} is due to the bending modes of Nb-O-Nb linkages [28] and the shoulder band at 815 cm^{-1} can be assigned to stretching vibrations of the peroxy groups [15, 18]. The peak at 229 cm^{-1} indicates the presence of Nb-OH bond, there were no other peaks noted, suggesting that no impurities were present.

3.2 Catalytic activity

Geraniol is an interesting substrate to be epoxidized to epoxy- or diepoxygeraniol. The selectivity to the desired epoxy must also be considered. In general, the epoxidation of geraniol occurs at the allylic double bond as was already observed by [29] and [13]. In this work, we used Nb_2O_5 and

ammonium tetraperoxonioate ($(NH_4)_3^+[Nb(O_2)_4]^-$) labeled Nb_2O_5/H_2O_2 . As can be seen from XRD, XPS and Raman spectroscopy, in the synthesis of this latter compound, the treatment of Nb_2O_5 with H_2O_2 did not modify the Nb_2O_5 structure and of peroxonioate species $[Nb(O_2)_4]^-$ was not observed. The formation of ammonium tetraperoxonioate ($(NH_4)_3^+[Nb(O_2)_4]^-$) was not evidenced in this work, as indicated by XRD, XPS and Raman. However, Nb_2O_5 treated with H_2O_2 promotes the formation of peroxy species on the Nb_2O_5 surface, which may be related to its catalytic behavior. The new sites on this catalyst should favor the epoxidation reaction. Table 2 summarizes the results obtained for the catalytic activity, expressed in terms of conversion and selectivity to citral, allyl epoxide and others, which were the only products obtained in all cases. To corroborate if the epoxidation is going in the absence of catalyst, blank experiments (without catalyst) were carried out.

Table 2 Selectivity and activity obtained for the oxidation of geraniol over Nb_2O_5 and Nb_2O_5/H_2O_2 catalysts

Catalysts	Conversion, %	Selectivity,		
		Citral	Allyl epoxide	Others
Nb_2O_5	20	7	86	7
Nb_2O_5/H_2O_2	17	14	80	6
None	<1	25	46	28

The main product obtained was allyl epoxide in all catalysts studied. No significant differences were observed in the catalytic activity using Nb_2O_5 treated with H_2O_2 , which can be attributable to the amount of H_2O_2 used during the synthesis of Nb_2O_5/H_2O_2 . The high selectivity at the allyl epoxide is due to the oxidation of the conjugated C=C double bond and the carbonyl function, respectively [see

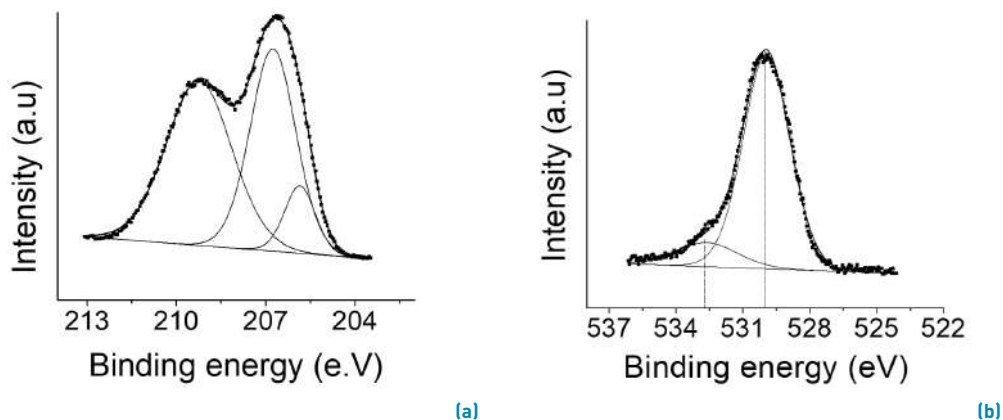


Figure 3 XPS profiles for Nb 3d (left) and O 1s (right) spectral lines of Nb_2O_5/H_2O_2 catalyst

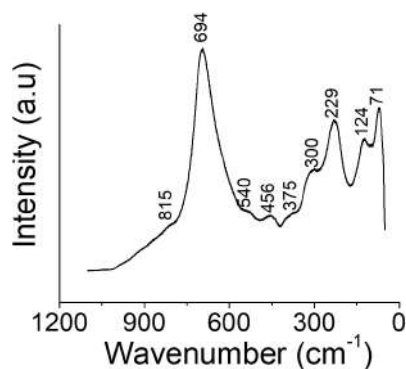


Figure 4 Raman spectra for the Nb_2O_5/H_2O_2 synthesized

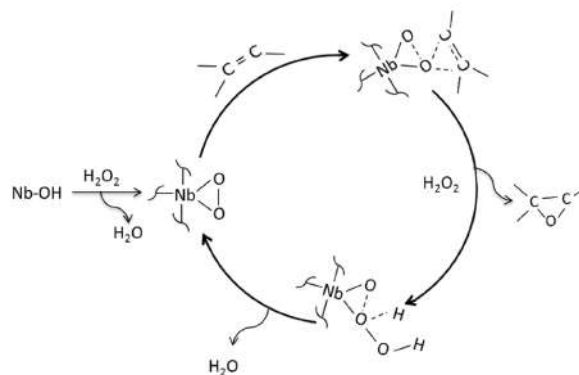


Figure 5 Proposed Geraniol oxidation pathway

Figure 5). The epoxide selectivity should be generated at peroxy sites and electronic structure assumptions, which is confirmed because the most nucleophilic group C=C double bond in the geraniol molecule is predominantly epoxidized [30], thus, the differences in selectivity observed is, at least in part, due to conversion «the higher the conversion, the higher epoxide selectivity», when is compared under the same reaction conditions. The other compounds are the sum of the other epoxide and glycols formed by the reaction between epoxides and H_2O in the Lewis acid sites. Recently, Nowak and colleagues reported that the catalytic properties of niobium-based catalysts are very sensitive to the type of support used. In this study, the best result was 60% selectivity to all epoxides using Nb(Co)SBA-15 as catalyst [31].

To evaluate the effect of solvent during the product extraction, the oxidation of geraniol over the Nb_2O_5/H_2O_2 catalyst was tested in different solvents (see Table 3). The conversion decreases as the dielectric constant of solvents decreases when acetonitrile, dichloromethane and dioxane were used as solvent, while using methanol,

the conversion increases between 2 and 3 times compared with the other solvents. This phenomenon can be explained because methanol is capable to form hydrogen bonds, which increases the epoxide extraction obtaining a more efficient catalytic system.

Table 3 Conversion using different solvents for the oxidation of geraniol over Nb_2O_5/H_2O_2 catalyst

Solvent	Dielectric Constant (k)	Conversion* %
Methanol	33	17
Acetonitrile	37	7
Dichloromethane	9.1	6
Dioxane	2.3	5

*After 4 h

The effect of the stirring speed in the range from 200 to 600 rpm was studied (not shown). In a typical profile, the initial rate increase as a function of stirring speed;

however, no significant effect on the rate was observed at stirring rates over 600 rpm, indicating the absence of mass transfer resistance.

To determine the order of reaction, the results were expressed as $\log r_0$ vs $\log[C_{\text{GERANIOL}}]$. The initial rates were calculated using a third-order polynomial equation, during the consumption of geraniol with the reaction time. The dependence respect to geraniol (reaction order) varied from 0.8 to 1.1, but it depends on the temperature employed. It was reported that during the oxidation of benzyl alcohol over tungstic acid describes similar results, it was found a first-order dependence with respect of benzyl alcohol concentration (BzOH) and completely independent respect to the H_2O_2 concentration used [32].

The formation of peroxo sites occurs after prolonged contact of time between the niobium surfaces with H_2O_2 . In addition, a high efficiency during the activation of these peroxo sites using H_2O_2 was observed during the progress of reaction. This effect is expected due to the reaction zero order obtained for H_2O_2 , confirming that high amounts of H_2O_2 are necessary to lead the reaction.

A proposed mechanism pathway for the oxidation of geraniol involves the activation and/or formation of peroxo sites by the reaction between H_2O_2 and Nb_2O_5/H_2O_2 (see Figure 5). The nucleophilic allylic olefin group on geraniol molecule attacks the electrophilic oxygen of the Nb-peroxo group in a concerted oxygen-transfer step, forming a three-membered-ring transition state, which gives the allylic epoxide [33], as it is observed in Figure 5. In fact, a reaction order of one with respect to geraniol can consider the reaction between the peroxo sites and geraniol as the rate-controlling step.

The initial catalytic activity was recovered when the catalyst used was treated in the same way as is described in experimental part.

4. Conclusions

The activation of Nb_2O_5 catalyst with H_2O_2 favors the peroxo-sites formation more than peroxoniobate isolates species on the surface. The formation of peroxo sites is essential in Nb_2O_5 bulk for the geraniol epoxidation that is conducted by the formation of a three-membered-ring transition state that gives the good selectivity to the allylic epoxide. Surface modification is the key issue for controlling the product distribution in the oxidation of geraniol. No change in the textural and morphologic properties were evidenced by treating Nb_2O_5 with H_2O_2 . The oxidation reaction is of first order with respect to the geraniol concentration and order zero with respect to H_2O_2 concentration.

5. Acknowledgements

We would like to thank VIE-UPTC for the financial support under the project SGI-2369.

References

- [1] A. Maniatakou and *et al.*, "Synthesis, structural and DFT studies of a peroxo-niobate complex of the biological ligand 2-quinaldic acid," *Polyhedron*, vol. 27, no. 16, pp. 3398-3408, Nov. 2008.
- [2] C. R. Waidmann, A. G. DiPasquale, and J. M. Mayer, "Synthesis and reactivity of oxo-peroxo-vanadium(v) bipyridine compounds," *Inorg. Chem.*, vol. 49, no. 5, pp. 2383-2391, Jan. 2010.
- [3] L. C. Passoni, M. R. H. Siddiqui, A. Steiner, and I. V. Kozhevnikov, "Niobium peroxo compounds as catalysts for liquid-phase oxidation with hydrogen peroxide," *J. Mol. Cat. A: Chem.*, vol. 153, no. 1-2, pp. 103-108, Mar. 2000.
- [4] L. C. A. Oliveira and *et al.*, "Pure niobia as catalyst for the oxidation of organic contaminants: Mechanism study via ESI-MS and theoretical calculations," *Chem. Phys. Lett.*, vol. 446, no. 1-3, pp. 133-137, Sep. 2007.
- [5] L. J. Burcham, J. Datka, and I. E. Wachs, "In situ vibrational spectroscopy studies of supported niobium oxide catalysts," *J. Phys. Chem.*, vol. 103, no. 29, pp. 6015-6024, Jun. 1999.
- [6] D. Bayot, B. Tinant, and M. Devillers, "Water-soluble niobium peroxo complexes as precursors for the preparation of Nb-based oxide catalysts," *Catal. Today*, vol. 78, no. 1-4, pp. 439-447, Feb. 2003.
- [7] M. Kantcheva, H. Budunoğlu, and O. Samarskaya, "Characterization of $Zr_6Nb_2O_{17}$ synthesized by a peroxo route as a novel solid acid," *Catal. Commun.*, vol. 9, no. 5, pp. 874-879, Mar. 2008.
- [8] A. Esteves and *et al.*, "New materials based on modified synthetic Nb_2O_5 as photocatalyst for oxidation of organic contaminants," *Catal. Commun.*, vol. 10, no. 3, pp. 330-332, Dec. 2008.
- [9] K. T. G. Carvalho, A. C. Silva, L. C. A. Oliveira, M. Gonçalves, and Z. M. Magriotis, "Nióbia sintética modificada como catalisador na oxidação de corante orgânico: utilização de H_2O_2 e O_2 atmosférico como oxidantes," *Quím. Nova*, vol. 32, no. 6, pp. 1373-1377, 2009.
- [10] T. C. Ramalho and *et al.*, "The molecular basis for the behaviour of niobia species in oxidation reaction probed by theoretical calculations and experimental techniques," *Mol. Phys.*, vol. 107, no. 2, pp. 171-179, Oct. 2010.
- [11] L. C. A. Oliveira, M. Gonçalves, D. Q. L. Oliveira, A. L. N. Guarieiro, and M. C. Pereira, "Síntese e propriedades catalíticas em reações de oxidação de goethitas contendo nióbio," *Quím. Nova*, vol. 30, no. 4, pp. 925-929, Aug. 2007.
- [12] M. Ziolek and *et al.*, "Catalytic performance of niobium species in crystalline and amorphous solids—gas and liquid phase oxidation," *Appl. Catal. A: Gen.*, vol. 391, no. 1-2, pp. 194-204, Jan. 2011.
- [13] N. Marin and *et al.*, "Control of the chemoselectivity in the oxidation of geraniol over lanthanum, titanium and niobium catalysts supported on mesoporous silica MCM-41," *Top. Catal.*, vol. 55, no. 7-10, pp. 620-624, Jul. 2012.
- [14] N. T. Prado and *et al.*, "Modified niobia as a new catalyst for selective production of dimethoxymethane from methanol," *Energy & Fuels*, vol. 24, no. 9, pp. 4793-4796, Aug. 2010.
- [15] N. Marin and *et al.*, " Nb_2O_5 as heterogeneous catalysts for the selective oxidation of geraniol," *Curr. Org. Chem.*, vol. 16, no. 23, pp. 2797-2801, 2012.
- [16] X. Secordel and *et al.*, " TiO_2 -supported rhenium oxide catalysts for methanol oxidation: Effect of support texture on the structure and reactivity evidenced by an operando raman study," *Catal. Today*, vol. 155, no. 3-4, pp. 177-183, Oct. 2010.
- [17] C. M. de Souza, S. C. de Souza, E. Roditi, and G. Gelbard, "Oxidations of benzyl alcohol by hydrogen peroxide in the presence of complexed peroxoniobium (V) species," *J. Chem. Res. [S]*, no. 3, pp. 92-93, 1997.
- [18] G. Haxhillazi, "Preparation, structure and vibrational spectroscopy

- of tetraperoxo complexes of Cr^{V+}, V^{V+}, Nb^{V+} and Ta^{V+}," Ph.D. dissertation, Siegen Univ., Siegen, Germany, 2003.
- [19] L. Dragone, P. Moggi, G. Predieri, and R. Zannoni, "Niobia and silica-niobia catalysts from sol-gel synthesis: an X-ray photoelectron spectroscopic characterization," *Appl. Surf. Sci.*, vol. 187, no. 1-2, pp. 82-88, Feb. 2002.
- [20] T. C. Ramalho and *et al.*, "The molecular basis for the behaviour of niobia species in oxidation reaction probed by theoretical calculations and experimental techniques," *Mol. Phys.*, vol. 107, no. 2, pp. 171-179, 2009.
- [21] F. J. Wong, N. Hong, and S. Ramanathan, "Orbital splitting and optical conductivity of the insulating state of NbO₂," *Phys. Rev. B*, vol. 90, no. 11, pp. 115 135-1-115 135-8, Sep. 2014.
- [22] A. Darlinski and J. Halbritter, "On angle resolved x-ray photoelectron spectroscopy of oxides, serrations, and protusions at interfaces," *Vac. Sci. & Technol. A.*, vol. 5, no. 4, pp. 1235-1240, 1987.
- [23] A. B. Posadas, A. O'Hara, S. Rangan, R. A. Bartynski, and A. A. Demkov, "Band gap of epitaxial in-plane-dimerized single-phase NbO₂ films," *Appl. Phys. Lett.*, vol. 104, pp. 0 929 011-09 290 112, 2014.
- [24] Y. Gao, Y. Liang, and S. A. Chambers, "Synthesis and characterization of Nb-doped TiO₂(110) surfaces by molecular beam epitaxy," *Surf. Sci.*, vol. 348, no. 1-2, pp. 17-27, Mar. 1996.
- [25] V. V. Atuchin, I. E. Kalabin, V. G. Kesler, and N. V. Pervukhina, "Nb 3d and O 1s core levels and chemical bonding in niobates," *J. Elect. Spect. Rel. Phenom.*, vol. 142, no. 2, pp. 129-134, Feb. 2005.
- [26] P. Chagas and *et al.*, "A novel hydrofobic niobium oxyhydroxide as catalyst: Selective cyclohexene oxidation to epoxide," *Appl. Catal. A: Gen.*, vol. 454, pp. 88-92, Mar. 2013.
- [27] B. X. Huang, K. Wang, J. S. Church, and Y. S. Li, "Characterization of oxides on niobium by raman and infrared spectroscopy," *Electr. Acta.*, vol. 44, no. 15, pp. 2571-2577, 1999.
- [28] A. A. McConnell, J. S. Aderson, and C. N. R. Rao, "Raman spectra of niobium oxides," *Spect. Acta Part A: Mol. Spect.*, vol. 32, no. 5, pp. 1067-1076, 1976.
- [29] F. Somma, A. Puppinato, and G. Strukul, "Niobia-silica aerogel mixed oxide catalysts: Effects of the niobium content, the calcination temperature and the surface hydrophilicity on the epoxidation of olefins with hydrogen peroxide," *Appl. Catal. A: Gen.*, vol. 309, no. 1, pp. 115-121, Jul. 2006.
- [30] J. M. de S. e Silva, F. S. Vinhado, D. Mandelli, U. Schuchardt, and R. Rinaldi, "The chemical reactivity of some terpenes investigated by alumina catalyzed epoxidation with hydrogen peroxide and by DFT calculations," *J. Mol. Cat. A: Chem.*, vol. 252, no. 1-2, pp. 186-193, Jun. 2006.
- [31] A. Feliczak, A. Wawrzyńczak, and I. Nowak, "Selective catalytic oxidations of cyclohexene, thioether and geraniol with hydrogen peroxide. sensitivity to the structure of mesoporous niobosilicates," *Micropor. Mesopor. Mater.*, vol. 202, pp. 80-89, Jan. 2015.
- [32] M. P. Chaudhari and S. B. Sawant, "Kinetics of heterogeneous oxidation of benzyl alcohol with hydrogen peroxide," *Chem. Eng. J.*, vol. 106, no. 2, pp. 111-118, Feb. 2005.
- [33] A. M. Al-Ajlouni, O. Saglam, T. Diafla, and F. E. Kuhn, "Kinetic studies on phenylphosphopolyperoxotungstates catalyzed epoxidation of olefins with hydrogen peroxide," *J. Mol. Cat. A: Chem.*, vol. 287, no. 1-2, pp. 159-164, May 2008.